Generation of dc Magnetic Fields by Rectifying Nonlinear Whistlers

R. L. Stenzel and J. M. Urrutia
Department of Physics and Astronomy, University of California, Los Angeles, California 90095-1547
(Received 13 May 1998)

A magnetic loop antenna, immersed in a laboratory plasma, excites whistlers whose wave magnetic field exceeds the ambient dc field and forms magnetic null points. The propagation becomes amplitude and polarity dependent. A time-average dc magnetic field is generated with an applied ac magnetic field of zero mean. [S0031-9007(98)07020-3]

PACS numbers: 52.35.Mw, 52.35.Hr, 52.40.Fd, 52.70.Ds

The generation of dc magnetic fields in plasmas is a topic of broad interest in space and laboratory plasma physics. Magnetic fields can be produced by various mechanisms such as fluid motions (dynamos [1,2]), gradients in temperature and densities (baroclinic effect [3–5]), nonlinearities in the Lorentz force for intense rf fields (laser-matter interactions [6,7]) or fluid turbulence (reverse-field pinches [8]). In the present Letter, we report experimental observations of dc magnetic fields generated by nonlinear whistler waves excited with a loop antenna in a high beta plasma. In general, nonlinearities arise when a wave modifies those plasma parameters which determine its propagation. For whistlers, these are density, magnetic field, and electron temperature. Density perturbations are known to cause filamentation of whistlers [9–11]. Rapid electron heating leads to conductivity changes and current filaments [12]. Here we consider magnetic perturbations by strong whistler vortices [13] with axial wave magnetic fields comparable to the ambient dc magnetic field. Simply, whistlers propagate faster when the wave field adds to the ambient field and slower when it opposes the dc field, in particular, when magnetic null points are created. The dependence of $\mathbf{B}(\mathbf{r}, t)$ on polarity and amplitude produces a nonlinear distortion in the waveform. While the applied magnetic field has a periodic waveform without a dc component, the plasma field contains a significant dc component as well as a new spectrum of harmonics. The plasma nonlinearity "rectifies" the applied magnetic field or induced currents. The underlying mechanism is, of course, the nonlinear Lorentz term, $\mathbf{v}(B) \times \mathbf{B}$, which governs the penetration of magnetic fields into electron MHD (EMHD) plasmas [$\partial\mathbf{B}/\partial t = \nabla \times (\mathbf{v} \times \mathbf{B})$] via low frequency whistlers [$\omega/k = (c/\omega_p)(\omega\omega_c \cos\theta)^{1/2}$] [14].

The experiment is performed in a 1-m-diam, 2.5-m-long pulsed discharge plasma sketched in Fig. 1. An electrostatically shielded magnetic loop antenna (12 cm diam, four turns) with dipole axis along $\mathbf{B}_0$ excites time-varying magnetic fields, $\mathbf{B}(\mathbf{r}, t)$, measured with a magnetic probe both in the absence and presence of plasma. The probe consists of three orthogonal 1-cm-diam, multiturn (30) loops, inside a grounded coaxial shield with a radial slot. In addition, the shield is electrically insulated from the plasma, making the probe insensitive to electrostatic signals. Applied repetitive current pulses (130 A, $\Delta t \simeq 10\ \mu$s, $t_{\text{rep}} \simeq 40\ \mu$s) of alternating sign produce peak dipole fields an order of magnitude larger than the ambient dc magnetic field, thereby creating magnetic null points/line in the vicinity of the antenna. The presence of the high-β [$\beta = nkT_e/(B_0^2/2\mu_0) \simeq 3$] plasma substantially modifies the applied potential fields.

The magnetic field topology is explained with the help of Fig. 2, which displays a snapshot of (B_y, B_z) in the y-z plane along the axis of the loop antenna ($x = 0$). The total field can be decomposed into three contributions: (i) the uniform dc field inside the plasma, $B_{0,z} \simeq 3.5$ G, (ii) the vacuum (potential) field of the dipole $\mathbf{B}_d(\mathbf{r}, t)$, and (iii) the field created by induced plasma currents, $\mathbf{B}_{\text{pl}}(\mathbf{r}, t)$. The latter is obtained from the difference of the measured fields in plasma and vacuum, $\mathbf{B}_{\text{pl}}(\mathbf{r}, t) = \mathbf{B}_{\text{plasma}}(\mathbf{r}, t) - \mathbf{B}_d(\mathbf{r}, t)$. When the dipole is aligned with $\mathbf{B}_0$ (Fig. 2a), the fields add inside the loop to form a strong mirror of ratio $B_{\max}/B_0 \geq 10$, but subtract outside to form a null line around the loop (not shown). When the axial dipole field opposes the dc field, a three-dimensional (3D) magnetic null point is created on axis at equal distances from the loop antenna (Fig. 2b). Field lines traced through the cusp clearly show the spine and fan of the separatrix. The field pattern of Fig. 2 is shown at the time of the current extrema ($dI_{\text{loop}}/dt \simeq 0$), where the induced plasma currents are small compared to the antenna current. However, during the current rise/fall the

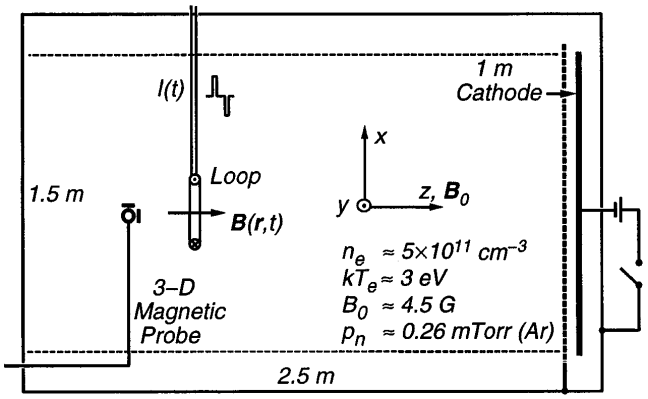

FIG. 1. Experimental setup.

 0031-9007/98/81(10)/2064(4)$15.00

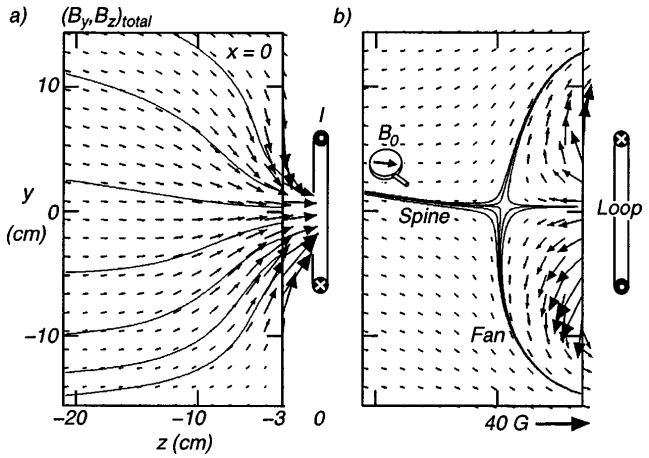

FIG. 2. Magnetic field (B_y, B_z) in the y-z plane along the dipole axis at the peak antenna currents. (a) Mirror topology produced by the positive current pulse; (b) null point topology due to the negative pulse.

plasma produces, in accordance with Lenz's law, dipolar fields opposing/adding to the applied one. In EMHD, the plasma also produces a linked toroidal field component $B_\theta[= \mp B_x(0, y, \pm z)]$ (not shown here). Thus, the plasma field has the topology of a 3D vortex [13,15]. Theoretically, vortex solutions have been derived from $\partial\mathbf{B}/\partial t = \nabla \times (\mathbf{v} \times \mathbf{B})$, which describes fields frozen into the electrons of fluid velocity $\mathbf{v}$ [16]. Small amplitude perturbations ($B_{\rm pl} \ll B_0$) propagating with wave velocity $v_\parallel = E/B_{\rm pl}$ along $\pm\mathbf{B}_0$ have $\mathbf{v}/v_\parallel = \pm\mathbf{B}_{\rm pl}/B_0$. Their current density, $\mathbf{J} = -ne\mathbf{v} = \nabla \times \mathbf{B}_{\rm pl}/\mu_0$, magnetic field, $\mathbf{B}_{\rm pl} = \nabla \times \mathbf{A}_{\rm pl}$, and vector potential, $\mathbf{A}_{\rm pl}$ (Coulomb gauge), are parallel/antiparallel to each other; hence their helicity densities, $\mathbf{A}_{\rm pl} \cdot \mathbf{B}_{\rm pl}$ and $\mathbf{J} \cdot \mathbf{B}_{\rm pl}$, are positive/negative (right-/left-handed twists or linkage [17]), for propagation along/opposite to $\mathbf{B}_0$. In the present experiment, both the dipole field and the plasma fields are larger than the uniform background field, such that the vortices become nonlinear.

The time dependence of the magnetic field is demonstrated for just one component, $B_{{\rm pl},x}(t)$, at one location, $x = 0$, $y = -3$ cm, $z = -6$ cm. There, $B_{{\rm pl},x}(t) = B_{{\rm plasma},x}(t)$ since $B_d(t) = 0$. Figure 3 shows the field produced by plasma currents, i.e., the difference between the fields measured in plasma and vacuum. The applied current or potential fields have symmetric waveforms with zero mean. The induced field is also symmetric with a negligible dc value for small antenna currents (Fig. 3a). However, for large antenna currents (Fig. 3b), the induced magnetic field is highly distorted with respect to current polarity and current rise and fall. The nonlinearity of the medium produces not only a dc field ("rectification") but also a rich spectrum of harmonics (Fig. 3c). For purpose of comparison, the spectral lines are normalized to the fundamental frequency, $\omega_0 = 2\pi/t_{\rm rep}$. While the spectrum of the current or applied field contains only odd harmonics, the spectrum of the magnetic field, $B_{{\rm pl},x}(\omega)/B_{{\rm pl},x}(\omega_0)$, exhibits a strong dc component and many even and odd harmonics.

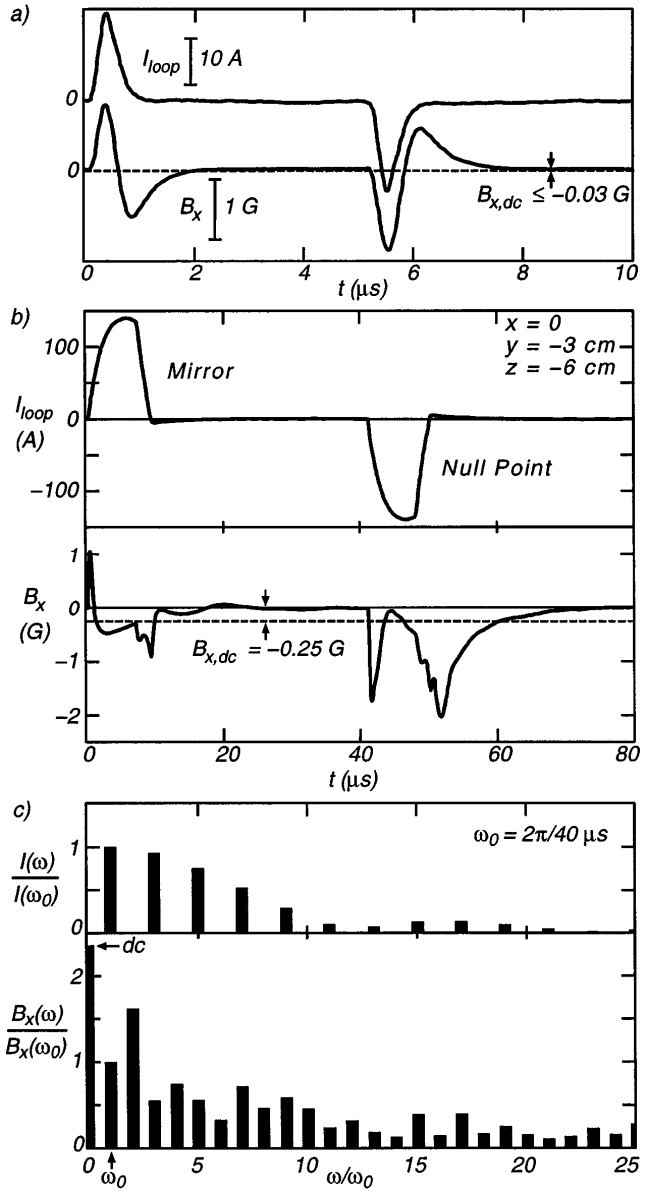

FIG. 3. Time dependence and spectra of antenna current and field component B_x ($= B_\theta$ for $x = 0$) produced by plasma currents. (a) Fields excited by small current pulses exhibit a negligible dc value. (b) Nonlinear field produced by large current pulses. (c) Spectra of the large antenna current (top) and induced magnetic field (bottom). Note that the former has no dc component or even harmonics, but the latter has both.

In order to analyze the cause of the nonlinearity, we start with the radial electron drift $\mathbf{E} \times \mathbf{B}$ inside the antenna created by the inductive electric field E_θ ($\propto -dI_{\rm loop}/dt$) and the axial magnetic field B_z ($\propto I_{\rm loop}$). The incompressible electrons stream out along the antenna axis, creating a current J_z and linked field B_θ. In the linear case, $B_z = B_0 = \text{const}$, and the drifts, currents, and

fields oscillate with zero mean. In the present case, the axial field differs during the current rise and fall. For example, at the location corresponding to Fig. 3, the axial field is positive ($\| \mathbf{B}_0$) at the switch-on of the negative current pulse, but negative during the switch-off. Since both E_θ and B_z change sign, the drifts, currents, and field B_θ have the *same* sign for current rise and fall; hence a dc field is created. For the positive current pulse, the axial field does not change in direction but in magnitude, such that B_θ also has a nonzero mean.

In general, the mean values of the plasma-generated fields for the positive and negative antenna pulses do not cancel. One reason is the different field penetration into the plasma with pulse polarity. In the magnetic mirror configuration, the whistler wave packet propagates along diverging field lines. In the null point geometry, all field lines created by the antenna have to undergo reconnection to penetrate beyond the volume bounded by the separatrix. The flux pileup associated with slow reconnection creates larger fields for longer times than those associated with a rapidly propagating whistler wave. This can be quantified by calculating the time rate of change of the magnetic flux near the antenna, $\partial\Phi/\partial t = \int(\partial B_z/\partial t)2\pi r\, dr$. Figure 4a shows that during the switch-off, the flux decay for the null point topology is twice as slow as for the mirror field geometry and 3 times slower than in vacuum. During the current turn-on, there is little difference between the two pulse polarities since it takes time to establish a null point in the plasma. Figures 4b and 4c show the propagation of the plasma-generated field component, $B_{\mathrm{pl},z}(x,t)$, on axis ($x = y = 0$) for both pulse polarities. The positive current pulse, which produces the mirror field, excites a rapidly propagating whistler transient both at the current rise and fall (Fig. 4b). For the negative pulse which establishes the magnetic null point, the field propagates at turn-off much slower than for the positive pulse. At turn-on, the propagation is faster than at turn-off since the perturbation propagates ahead of the null point. The slow propagation in the presence of a null point is qualitatively explained by the dependence of the whistler speed on the total field strength, $v_\| \propto B^{1/2}$. Note that the present whistler wave is so large that it carries the null point along well after the end of the antenna current pulse.

The nonlinearity of the plasma currents/fields varies with location. At all measured positions, the time averages of the plasma-generated field, $\langle \mathbf{B}_{\mathrm{pl}}(\mathbf{r},t)\rangle_t$ have been calculated (the antenna vacuum field has zero mean and $B_0 = \mathrm{const}$). Figure 5 shows vector fields in two orthogonal planes separately for each antenna pulse as well as the sum of both pulses. In the x-y plane, the negative pulse (Fig. 5b) produces a dc field dominated by a negative component as explained for Fig. 3b. In the y-z plane, there is a significant axial dc field produced by flux pileup. The positive pulse (Fig. 5a) produces a transverse field with predominantly positive B_θ because the smaller axial field at the pulse turn-on leads to a stronger $\mathbf{E} \times \mathbf{B}$ drift than at turn-off. Since the nonlinearities for the two pulse polarities are different, the net dc field exhibits a complicated multipole configuration (Fig. 5c) with little similarity to the applied dipole field. It is interesting to note that the dc magnetic field contains essentially no net helicity. The spatial structure of harmonics can also be obtained but is beyond the scope of this Letter.

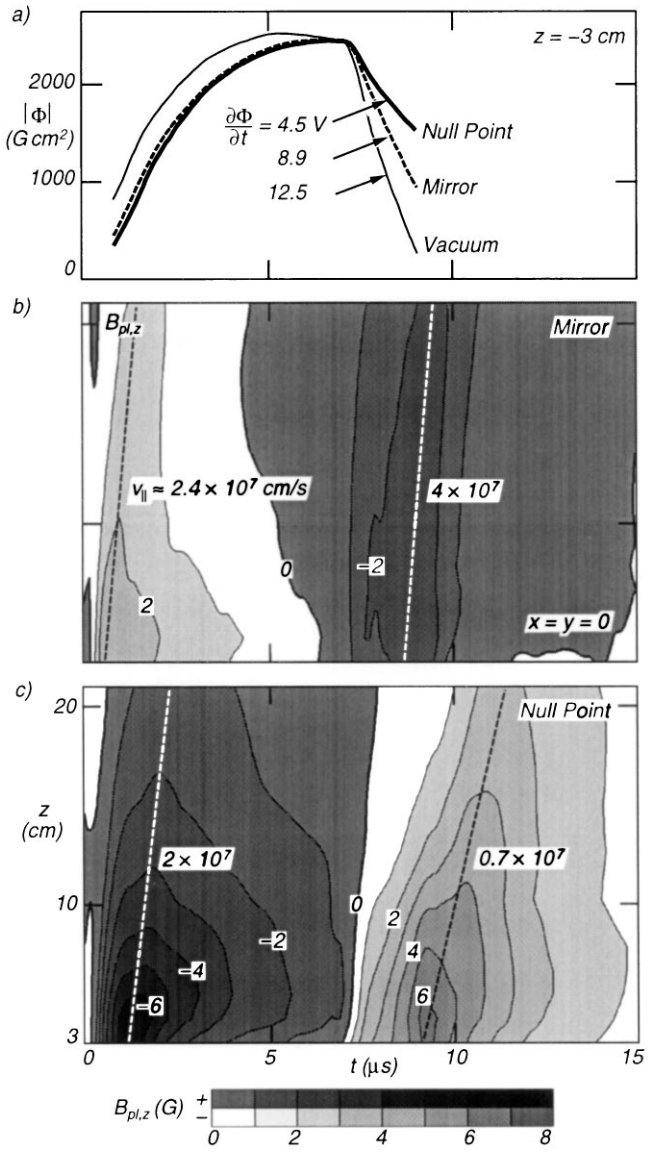

FIG. 4. (a) Magnetic flux at $z = -3$ cm in vacuum and plasma. Note slow decay in the presence of a magnetic null point. Contours of the plasma-produced field component, $B_{\mathrm{pl},z}$, in the axial z-t plane for (b) mirror and (c) null point topology. Whistler propagation speed depends on total axial magnetic field which varies with wave amplitude and sign.

In conclusion, a new nonlinear mechanism for generating dc fields from ac fields in plasmas has been presented. Aside from the intrinsic interest in nonlinear physics, the effect may occur in space plasmas for rapidly rotating or oscillating dipoles or large amplitude whistlers in high beta plasmas.

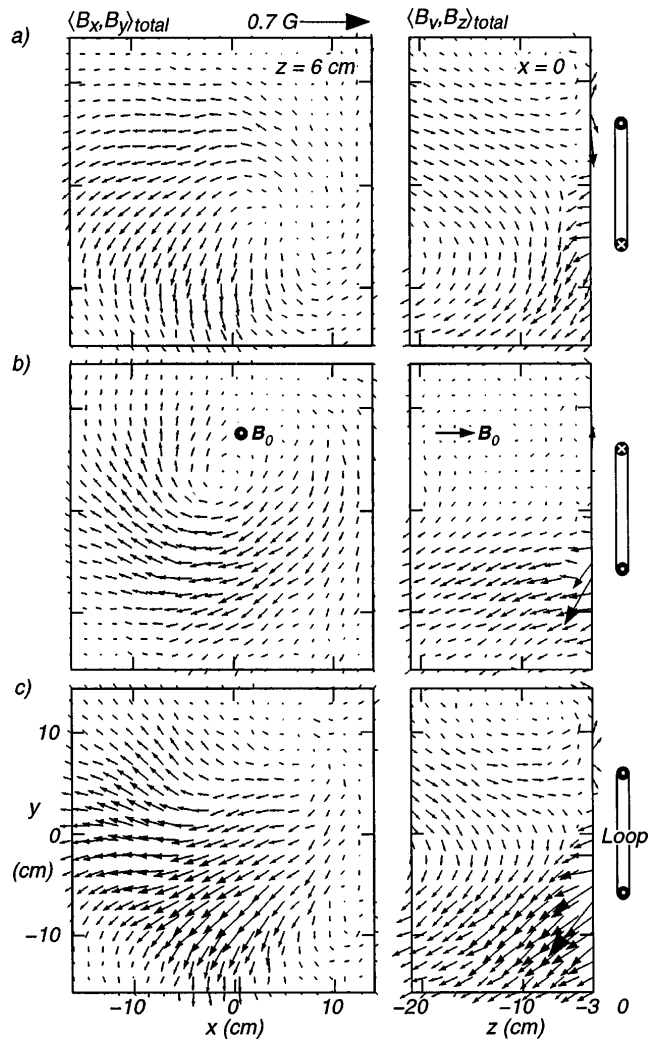

FIG. 5. Topology of the dc magnetic field shown as vector fields in two orthogonal planes, $\langle B_x, B_y \rangle (x, y)$ and $\langle B_y, B_z \rangle (y, z)$. The time average values are shown separately for (a) the positive pulse, (b) the negative pulse, and (c) for both pulses. The net dc field (c) has a multipole geometry unrelated to the dipolar antenna field.

The authors gratefully acknowledge support for this work by the National Science Foundation under Grant No. PHY97-13240.

[1] H. K. Moffat, *Magnetic Field Generation in Electrically Conducting Fluids* (Cambridge University Press, Cambridge, England, 1987).
[2] A. H. Boozer, Phys. Fluids B **5**, 2271 (1993).
[3] A. Kageyama and T. Sato, Phys. Rev. E **55**, 4617 (1997).
[4] J. A. Stamper and B. H. Ripin, Phys. Rev. Lett. **34**, 138 (1975).
[5] L. Stenflo and M. Y. Yu, Phys. Fluids **29**, 2335 (1986).
[6] A. M. Mirza, G. Murtaza, and P. K. Shukla, Phys. Plasmas **3**, 731 (1996).
[7] T. J. M. Boyd, in *International Conference on Plasma Physics*, edited by P. H. Sakanaka, E. Del Bosco, and M. V. Alves, AIP Conf. Proc. No. 345 (AIP, New York, 1995), pp. 238–246.
[8] H. Ji, S. C. Prager, A. F. Almagri, J. S. Sarff, Y. Yagi, Y. Hirano, K. Hattori, and H. Toyama, Phys. Plasmas **3**, 1935 (1996).
[9] B. G. Eremin and A. G. Litvak, JETP Lett. **13**, 430 (1971).
[10] R. L. Stenzel, Phys. Fluids **19**, 865 (1976).
[11] H. Sugai, M. Maruyama, M. Sato, and S. Takeda, Phys. Fluids **21**, 690 (1978).
[12] J. M. Urrutia and R. L. Stenzel, Phys. Plasmas **3**, 2589 (1996); **4**, 36 (1997).
[13] R. L. Stenzel, J. M. Urrutia, and C. L. Rousculp, Phys. Rev. Lett. **74**, 702 (1995).
[14] A. S. Kingsep, K. V. Chukbar, and V. V. Yan'kov, in *Reviews of Plasma Physics*, edited by B. Kadomtsev (Consultants Bureau, New York, 1990), Vol. 16, p. 243.
[15] C. L. Rousculp, R. L. Stenzel, and J. M. Urrutia, Phys. Plasmas **2**, 4083 (1995).
[16] M. B. Isichenko and A. M. Marnachev, Sov. Phys. JETP **66**, 702 (1987).
[17] M. A. Berger and G. B. Field, J. Fluid Mech. **147**, 133 (1984).